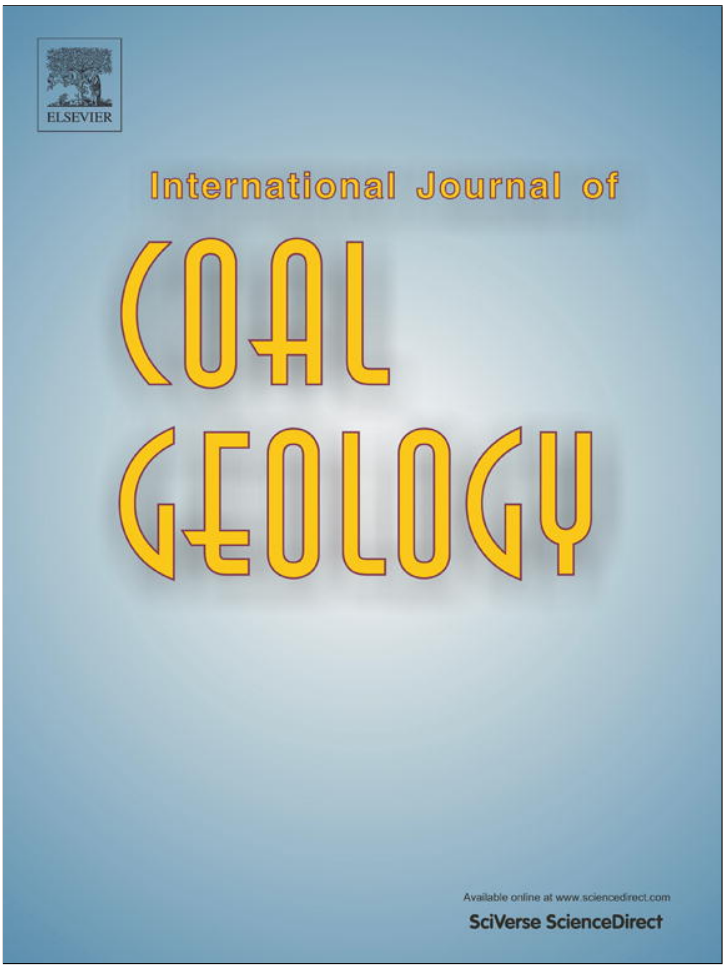

(This is a sample cover image for this issue. The actual cover is not yet available at this time.)

International Journal of Coal Geology 109–110 (2013) 24–35

Contents lists available at SciVerse ScienceDirect

International Journal of Coal Geology

journal homepage: www.elsevier.com/locate/ijcoalgeo

Spectrochemical study of coalified *Trigonocarpus grandis* (Pennsylvanian tree-fern ovule, Canada): Implications for fossil–organ linkage

Erwin L. Zodrow [a], Robert Helleur [b], Ulrike Werner-Zwanziger [c], Banghao Chen [c], José A. D'Angelo [a,d,e,*]

[a] *Palaeobotanical Laboratory, Cape Breton University, Sydney, Nova Scotia, Canada*
[b] *Department of Chemistry, Memorial University of Newfoundland, St. John's, Canada*
[c] *Department of Chemistry, Dalhousie University, Halifax, Nova Scotia, Canada*
[d] *Instituto Argentino de Nivología, Glaciología y Ciencias Ambientales (IANIGLA)-CCT-CONICET, Argentina*
[e] *Área de Química, Instituto de Ciencias Básicas, Universidad Nacional de Cuyo, Centro Universitario-M5502JMA-Mendoza, Argentina*

ARTICLE INFO

Article history:
Received 22 November 2012
Received in revised form 24 January 2013
Accepted 25 January 2013
Available online 7 February 2013

Keywords:
Histochemistry
Coalified ovules
Pyrolysates
Carboniferous

ABSTRACT

Five coalified ovules of the type *Trigonocarpus grandis* are investigated four of which co-occur with tree-fern foliage *Alethopteris pseudograndinioides* in the medullosalean forest (basal Cantabrian), and the fifth occurs in top Asturian D (Sydney Coalfield, Canada). Addressed are questions of variability (what is a coalified ovule?), comparison with petrified ovules, pyrolysates and the original make-up of the *grandis* seeds, and can similar chemistry proxy for organic connection between ovule and foliage?

The results demonstrate variable preservation quality despite similar thermal-maturity levels in the geological interval in which the ovules were collected. Nevertheless, the proposed *T. grandis* model is based on evidence from epidermises associated with inner and outer integuments, and a two-layered nucellus with granulose exine that is covered by a diaphanous layer (tectum?) and nucellar cuticle. The latter separates the inner cuticle of the inner integumentary surface from the megaspore membrane. Parenchymatous and sclerenchymatous cell structures are rare, whereas evidence for integuments, vasculature, and sclerotesta is equivocal. Overall, these features compare with petrified seeds.

^{13}C nuclear-magnetic resonance analysis suggests that the *A. pseudograndinioides* tree fern bore *T. grandis* seeds. Pyrolysates from low and high molecular weights can almost exclusively be grouped with alkenes and aromatics; phenolics, furan and branched alkenes; and with n-alkene/n-alkane homologous series (~3 to 1) for cuticles from the inner integumentary surface which suggests a cutin-based, aliphatic-rich biomacromolecule. More generally, preservation is presumed correlative with aliphatic content, but not exclusively, and organ–organ linkage by spectrochemical means certainly has potential as a new research vector in palaeobotany.

1. Introduction

Structure of North American pachytestal ovules (*Pachytesta* Brongniart) of Pennsylvanian age are well-known from sectioned coal balls (e.g., Darrah, 1968 and others; Hoskins and Cross, 1946; Taylor, 1965), and from Zimmerman and Taylor's (1970) scanning- and transmission-electron transmission images. In contrast, coalified Carboniferous trigonocarpalean ovules remain largely uninvestigated, except that Arnold (1948) studied cutinized *Trigonocarpus* Brongniart from the Michigan Basin, where "cutinized" is synonymous with fossilized-cuticle (Zodrow, 1977). His observations that "… these two protective layers [*sic* integumentary cuticle and nucellar epidermis] ….. retain the outlines of the integument cavity and the form of the nucellus" (Arnold, 1948, p. 138) served as guide for our investigative interpretation.

We studied five coalified ovules of the type *Trigonocarpus grandis* Lesquereux, 1884 (P821, pl 111, Figs. 1–3) emend. Cleal et al., 2010 from two successive coal seams in the Sydney Coalfield (Fig. 1). One ovule is from the older seam. The others co-occur with massive amounts of compressed foliage of *Alethopteris pseudograndinioides* Zodrow et Cleal, 1998 and *Linopteris obliqua* Zodrow et al., 2007. Foliage of these two medullosalean tree ferns absolutely dominate the fossil record at this open-pit coal mine (Zodrow, 2002, 2004, 2007), which is aptly named a lagerstätte for a medullosalean forest in the Canadian Carboniferous Maritimes. Concomitantly, the lagerstätte offers an opportunity for assessing the physical association between ovule–foliage (see organ–organ association: Meyen, 1984; Rothwell, 1985).

This study addresses the following questions: (i) what structure/tissue components of the original seed are preserved and what

* Corresponding author at: Instituto Argentino de Nivología, Glaciología y Ciencias Ambientales (IANIGLA)-CCT-CONICET-Mendoza, Avda. Ruiz Leal s/n Parque Gral. San Martín (5500) Mendoza, Argentina. Tel.: +54 261 5244255; fax: +54 261 5244201.
E-mail addresses: erwin_zodrow@cbu.ca (E.L. Zodrow), rhelleur@mun.ca (R. Helleur), ulrike.wernerzwanziger@gmail.com (U. Werner-Zwanziger), joseadangelo@gmail.com, joseadangelo@yahoo.com (J.A. D'Angelo).

0166-5162/$ – see front matter © 2013 Elsevier B.V. All rights reserved.
http://dx.doi.org/10.1016/j.coal.2013.01.013

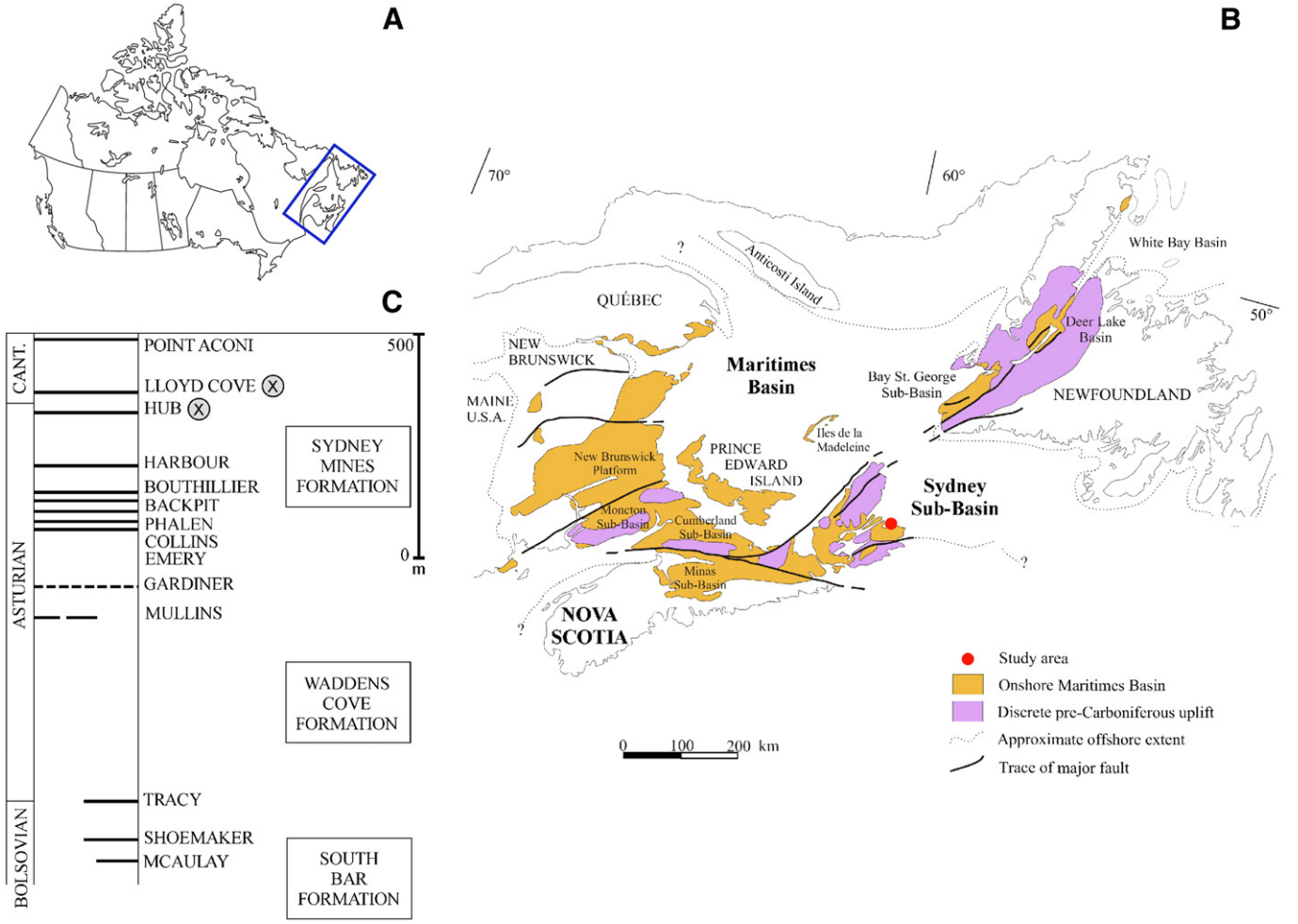

Fig. 1. Study location. (A) Canada. (B) Maritimes Basin with Sydney Coalfield (Sub-Basin), Nova Scotia. (C) Local coal stratigraphy. The two sampled coal seams are marked (X), and the medullosalean forest occurs in the roof rock of the Lloyd Cove Seam. CANT. = Cantabrian age (Zodrow and Cleal, 1985).

influences preservation variability? (ii) What was the original make-up of the seeds viewed through pyrolysates of selected components? (iii) What is the evidence for comparison with petrified pachytestal ovules, e.g. *P. gigantea*? We also advance the hypothesis that common chemistry of ovule–foliage proxies for organic connection, subject to certain conditions. Used in this instance are methods of ^{13}C CP/MAS NMR (Berns et al., 2011; Knicker, 2011). A synthetic model of the histochemistry of *T. grandis* will be published at a future date.

2. Ovular nomenclature

Medullosalean coalified ovules differ from medullosalean foliar compressions in two megascopical aspects: (1) they are much thicker, 10–60 times, than a general 30-μm pteridospermous compression with cuticle, and (2) structures are variably preserved as intercalated coaly and non-coaly layers. In its most simple representation, a medullosalean [fertilized] seed (Fig. 2) is comprised of an integument (seed-coat cover) surrounding the nucellus (*cf.* megasporangium) which contains the embryo. Durable cuticles separate/cover these components (Arnold, 1948; Oliver, 1903; Sporne, 1974, Fig. 3; Thomas and Spicer, 1987, and others), which in turn are covered by a structured diaphanous layer (tectum? cf. Zimmerman and Taylor, 1970, Pl. 6, Figs. 1 and 5). We follow van Bergen et al. (summary: 1994a) who used the term cuticle for describing unicellular integumentary layers of high-aliphatic content for angiospermous fossil water-plant seeds (cf. Cleal et al., 2010; Hoskins and Cross, 1946; Taylor, 1965; and Zimmerman and Taylor, 1970). We caution that it remains to be established if the cuticle from extant gymnospermous ovules, so named by Favre-Duchartre (1956) and De Sloover (1964), correlate

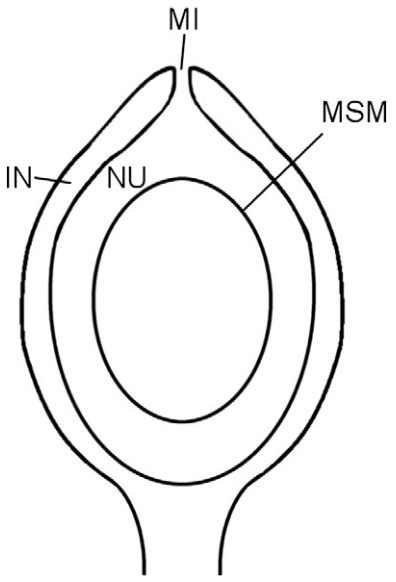

Fig. 2. Schematic longitudinal section of an ovule. MI = micropyle, IN = integuments, NU = nucellus, and MSM = megaspore membrane.

with what we refer to as cuticle in this paper, which actually represents an epidermis.

3. Material and background of thermal maturity

Three-dimensional sandstone casts (cf. syntypes of *T. grandis*: Gastaldo and Matten, 1978, Figs. 3–5) are not known from Sydney. A flattened shaley cast with prominent tripartite ridges (Cleal et al., 2010, Pl. 1, Figs. 2–3), though, compares with the syntypes. Impressions of the Sydney ovules in the shaley matrix, 6–9 cm long and 4–6 cm wide, are reasonably complete dimension-wise, but of the brittle coaly compressions (300 μm to 1700 μm thick) less than 20% remain for analysis, generally.

Supportive of this investigation is Nomarski phase-contrast microscopy of more than 200 macerated structure/tissue fragments that are organized on 56 glass-covered slides: 20 for 5-6/8-1, 24 for 85-202, 8 for ovule 3-258a, 3 for 5-10/11-5, and 1 for 2-306. Four ovules, viz. 2-306, 3-258a, 5-10/11-5, and 5-6/8-1, originated from the roof rock of the Lloyd Cove Seam that entombs the medullosalean forest which was exposed in 200 m by 100 m open-pit mine, now a lake (Fig. 1C). Provenance of the fifth ovule, 85-202, is the roof rock of the Hub Seam (Fig. 1C), where it is a rare component among a Late Asturian D flora. Hereafter, 5-6/8-1 is referred to as 8-ovule (Fig. 3A), and 85-202 as 202-ovule (Fig. 3B and C).

Coal samples (vitrain) from the Lloyd Cove (2.4 m height) and the Hub (2.3 m height) seams are included in the analyses. Key references relating to petrography, mineralogy, and physicochemical characteristics of these seams are Birk (1990) and Hacquebard (1993, 1998). The banded, bituminous B, seams are dominated by bright coal (vitrain and clarain, up to 97%), high pyrite contents (total sulfur 4.7% and 5.7%, respectively; Zodrow, 1987), clay and other mineral classes. Although the seams are separated by a 121-m shale-sandstone Pennsylvavian cyclothem (Gibling and Bird, 1994), their thermal histories are comparable which is inferred from identical vitrinite-reflectance values (Ro% is 0.65%; Zodrow et al., 2009, Table 1; Hacquebard and Donaldson, 1970), confirmed by ^{13}C CP/MAS NMR analyses (Fig. 4). In contrast, Ro% values for 8-ovule range from 0.62% to 0.83% (mean = 0.72%, n = 20).

4. Methods

4.1. Chemical treatment, and names of sample forms

Schulze's (1855) oxidative process is used for macerating the ovules and foliage of *A. pseudograndinioides* to retrieve the study

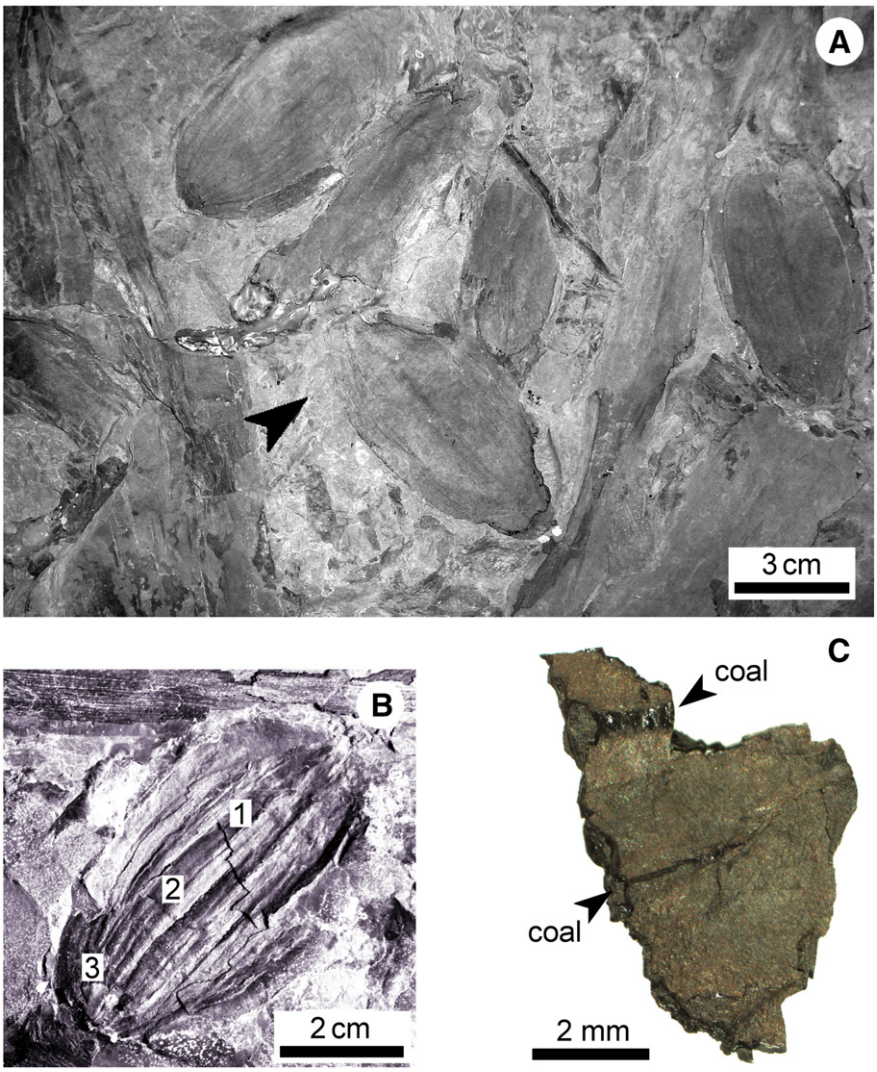

Fig. 3. *Trigonocarpus grandis*. 8-ovule and 202-ovule. (A) 8-ovule (arrowed) from the medullosalean forest. Detail of block 5-6/8-1 with eight detached ovules, Lloyd Cove Seam. (B) 202-ovule, where "1", "2" and "3" identify cupric V layers (sample name: Table 1, supplementary data). Hub Seam. (C) Detail of (B) showing one of the cupric V layer after HF liberation.

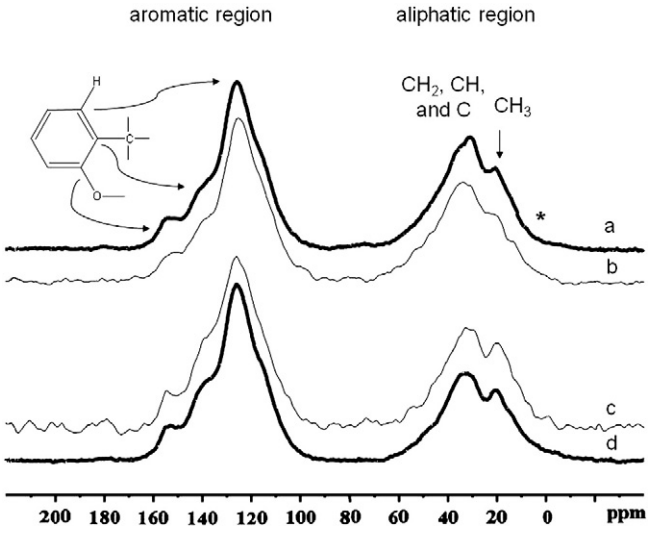

Fig. 4. ^{13}C CP/MAS NMR spectra of vitrain of the Lloyd Cove Seam (*a* and *c*) and Hub Seam (*b* and *d*); CP-contact times of 0.5 ms (a and b) and 1 ms (c and d). The star * identifies spinning side bands.

materials (see analytical details in D'Angelo et al., 2010a; Zodrow et al., 2012). The names of the sample forms (unmacerated hand specimens) are distinguished from structure/tissue component(s) that the forms yielded after maceration. One form did not need maceration, and the present form names are coordinated with those introduced by D'Angelo and Zodrow (2011, Fig. 3) (Table 1, supplementary material).

4.2. Py-GC/MS

Selected structures/tissues from 8-ovule, including the alkaline sample, 202-ovule and 3-258a were thermally fragmented to volatile-pyrolysis products (pyrolysates) as follows. A 0.5 mg sample loaded in a cup was quickly introduced into a Frontier Lab vertical micro-furnace pyrolyzer set at 650°C. The pyrolyzer is interfaced to an HP5890 GC equipped with an HP5971A MS. An Rtx-1301 column (60 m, 0.25 mm id, 1.4 μm) is used for the analysis of low molecular-weight (M.W.) pyrolytic products, whereas a DB-5ms column (30 m, 0.25 mm id and 0.25 μm) is used for the analysis of the higher boiling point alkenes/alkanes, higher M.W. The pyrolysis interface and GC injector are set at 280 °C and the MS interface at 290 °C, and column pressure is 15 psi and the split flow 20 mL min^{-1}. Oven-temperature program: 40 °C for 5 min then 7 °C min^{-1} to 240 °C, held for 5 min (for the Rtx-1301 column); 60 °C for 4 min then 5 °C min^{-1} to 280 °C, held for 5 min (for the DB-5ms column). The mass-spectrum scan ranges from m/z 34 to 350, and identifying pyrolysates are based on standards, or on NIST mass-spectrum library.

4.3. ^{13}C CP/MAS NMR experiments

Used was a Bruker Avance NMR spectrometer equipped with a 9.4 T magnet (Larmor frequency 400 MHz for ^{1}H and 100.65 MHz for ^{13}C). Finely powdered material (12.3 mg) of 8-ovule, 24.9 mg of cuticles of *A. pseudograndinioides*, and 73 mg for each vitrain sample from the Lloyd Cove and Hub Seams were packed into 4-mm rotors without further preparation. They were spun between 7.0 and 12.0 kHz to characterize the signal overlap of the spinning sidebands (SSB) with the isotropic shift peaks. All spectra shown were acquired at 12 kHz, and a recycle delay of 3 s was determined to be sufficient. The other parameters (proton decoupling) were optimized on glycine, whose carbonyl resonance also served as external, secondary chemical-shift standard at 176.06 ppm.

CP (cross-polarized)-contact time dependences on the aliphatic and aromatic signals influence the aromaticity fraction (see Werner-Zwanziger et al., 2005), but such a ratio taken with identical experimental conditions, as we have done, can be used to determine similarity between the Lloyd Cove and Hub Seam coals. The integral limits we used for the aromatic groups covered the well-separated experimental features between 170 ppm and 90 ppm. Spectra of 8-ovule and *A. pseudograndinioides* were acquired at 2 ms CP-contact times to enhance the weak aromatic signals. Spectra with good signal-to-noise ratios were acquired with 17,680 scans (Lloyd Cove), 20,500 scans (Hub Seam), 51,200 scans (8-ovule), and 14,336 scans (*A. pseudograndinioides*), for a total acquisition time of 43 h (Fig. 4).

5. Results

5.1. Structure/tissue summary

5.1.1. 8-ovule

One thick tissue layer was separable into seven surfaces (Fig. 5A to G). Fig. 5A presumably is an inner cuticle of the inner integument (folded-over) from which a structured, noncutinized diaphanous membranous layer is seen slipping off, diaphanous layer for short. Fig. 5B shows narrow-elongate rectangular sclerenchymatous cells (19–30 μm wide), but accurate length measurements are difficult to determine despite some cross walls (the implied sequential position is not certain). Fig. 5C–D and E–F document each a two-layered granulose megaspore membrane (exine: Taylor, 1965) characterized by variable cell shapes and sizes (70–300 μm long, 60–200 μm wide), including slightly elongate to near-isodiametric cells. Cuticle A (Fig. 5G, Table 1, supplementary data) shows 3–10 μm wide anticlinal walls (or borders of cells), and variable cellular topography of namely two conspicuous patterns. One of them constitutes single (33–43 μm wide and 73–126 μm long), doublet, or triplet rectangular cells that occur irregularly; the other near-isodiametric cells (43–53 μm by 46–56 μm) among them oval, pentagonal, or triangular cells. An imprint/overlay of a diaphanous layer is present with large irregularly shaped cells bounded by 1–3 μm wide curvilinear cell walls. Fig. 5G probably corresponds to Fig. 5A. A nucellar image (Fig. 5H) shows a megaspore membrane and brownish cutinized cuticular cell walls adhering to granulose exine; faint nucellar cells are near-isodiametric in shape.

5.1.2. 202-ovule

Consists of layers of vitrain intercalated with non-coaly layers, e.g., cupric V (Fig. 3C, Table 1, supplementary data), where cupric refers to copper content (D'Angelo and Zodrow, 2011). The variety of structure/tissue components macerated from cupric V, vitrain, and unoriented samples, are imaged in Figs. 6 to 8. Cupric V, Fig. 6A before and Fig. 6B after maceration, harbors three layers in original positions, referred to as "1" to "3". Layer "1", separated into two surfaces (Fig. 6C and D), is interpreted as covering the inner integument (itself not preserved). Both surfaces have moderately thick anticlinal walls, but differing cellular and diaphanous-layer topographies. Fig. 6C has occasional rectangular doublets (30–47 μm wide and 73 μm long) and near-isodiametric cells (30–44 μm wide and 37–47 μm long), together with subtriangular and pentangular five-sided cells; cells of the diaphanous layer (50–67 μm by 50–127 μm) are separated by ca. 1.5 μm wide anticlinal walls. In contrast, Fig. 6D only has occasional single rectangular cells (33 μm wide and 67 μm long), among predominating near-isodiametric cells (27–40 μm by 27–43 μm). The cells of the diaphanous layer tend to be larger (83 μm by 133 μm).

Layer "2" is separated into three distinct granulose megaspore membranes (Fig. 7A to C), where Fig. 7A is a thin exine surface, and Fig. 7B shows megaspore-membrane cells and also what appears to be adhering cutinized nucellus-cuticle material (62–152 μm by 57–152 μm). At ×500 magnification (Fig. 7C), the granulose-surface structure of

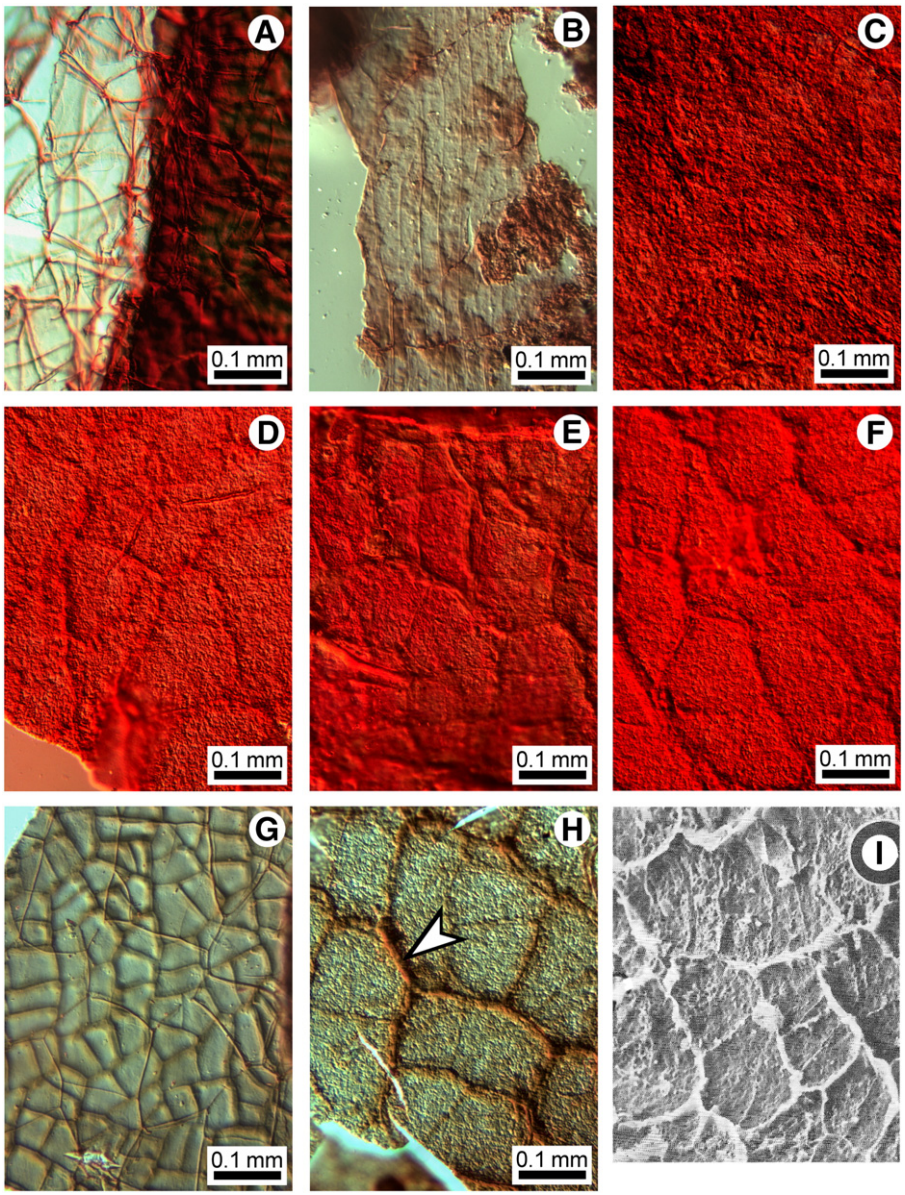

Fig. 5. *Trigonocarpus grandis*. 8-ovule. (A) Folded-over inner cuticle of the inner integument with the diaphanous layer sliding-off. Slide 05-6/8-1/2 (8-ovule). (B) Elongate cells of rib-related tissue. Slide 8ovule8L. (C) to (F). Granulose megaspore membranes. Slides 05-6/8-1/firstLay, 05-6/8-1/2Layer, 05-6/8-1/3Layer and 05-6/8-1/4Layer, respectively. (G) Equivalent to cuticle A, with diaphanous layer imprint. Slide 8ovule8C. (H) Type slide of the granulose megaspore membrane with adhering nucellar cuticle, arrowed, and outlines of nucellar cells. Slide 8ovule8E. Nomarski phase-contrast microscopy. (I) Scanning-electron micrograph of the megaspore membrane of *Pachytesta composita*. Source Zimmerman and Taylor (1970, Plate 2, Fig. 4 x178).

Fig. 7B remains unresolved. Oliver (1903, p. 472) who conjectured that similar-pitted structures in the nucellus of recent *Torreya* (Family: Taxaceae) performed a water-transfusion function. The inseparable two-surface cuticle "3" (Fig. 7D) is interpreted as covers (epidermises) of the outer integument. Cell topography consists of rare rectangular doublets (33–37 μm wide and 73–76 μm long), and near-isodiametric cells (33–47 μm wide and 37–57 μm) with moderately thick anticlinal walls, and faint imprints of the diaphanous layer.

Maceration products (101 h) of what a ca. 1 mm sized outer-vitrain fragment preserved, where sample size is limited by brittleness, are illustrated by parenchymatous tissue (Fig. 7E) whose square-like cells have cutinized anticlinal walls and very thin luminae, and sclerenchymatous cells (Fig. 7F), as suggested by the long and narrow cells (compare Figs. 5B, and 8C).

An unoriented 0.75-mm wide and 10-mm long linear structure with intact lateral margins is documented before (Fig. 8A) and after 73 h maceration (Fig. 8B). The structural linearity correlates with the elongate cells (49–114 μm long and 11–15 μm wide) that have relatively thick anticlinal walls both on the reverse and obverse surfaces that are parallel with the lateral margins (Fig. 8C; cf. Fig. 5B). An unoriented amber-colored sample form (Fig. 8D, HF-freed: no maceration) resembles a fossilized-cuticle (Zodrow and Mastalerz, 2007), but lacks cellular structure. We named it fossilized layer (Table 1, supplementary data).

5.1.3. 3-258a ovule

Repeated maceration of samples of the entire specimen only yielded a cuticle? (Fig. 9A) that has small, more or less near-isodiametric cells (22–84 μm by 30–50 μm). Megaspore membranes are not preserved.

5.1.4. 5-10/11-5 ovule

One single layer, after macerating the entire specimen, separated into a granulose megaspore membrane (Fig. 9B) without adhering nucellar cuticle, and presumably the inner cuticle of the inner

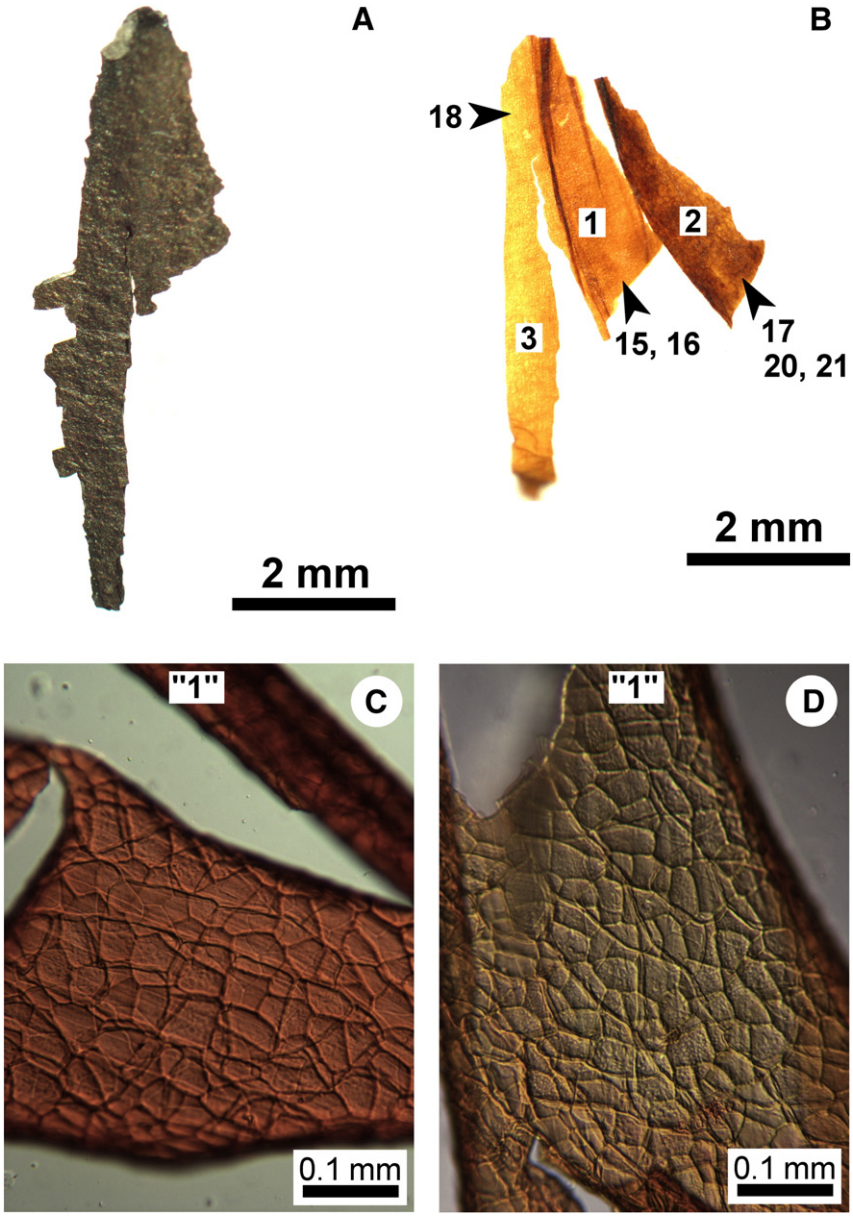

Fig. 6. *Trigonocarpus grandis*. 202-ovule. (A) Cupric V HF-liberated. (B) After 147 h maceration, surfaces "1, 2, and 3" are retrieved (see text), and "15-18, 20-21" are keyed to the slide numbers. (C) and (D) Inner/outer cuticles covering the inner integument. Slides 85-202/15 and 85-2002/16, respectively. (A) and (B) photographed immersed in water, and (C) and (D) by Nomarski phase-contrast microscopy.

integumentary surface (Fig. 9C). Cell topography includes relatively frequent rectangular doublets (30–36 μm long and 66–107 μm long), and near-isodiametric cells (33–54 μm wide and 42–67 μm long). Imprints of the diaphanous layer are not observed. We named it cuticle B (Table 1, supplementary data).

5.1.5. 2-306 ovule

Preserved tissue includes narrow elongate cells (cf. Fig. 8C), and nucellar cuticle still attached to a nucellar megaspore membrane with exine sculpture, not shown.

5.2. Py-GC/MS chromatograms

5.2.1. Cuticle A, 8-ovule

Fig. 10A and B represents low M.W. and higher M.W. pyrolytic products, respectively, where peak identification (1 to 10) is keyed to Table 2, (supplementary material). The low M.W. products (Fig. 10A) include isoprene(5), benzene(7) and related structures, e.g., toluene(1) whose precursor likely is coalified lignocellulose or lignin (Hatcher et al., 1989; Lyons et al., 1995), though other sources cannot be ruled out such as macromolecule-bound diaromatic carotenoids (Hartgens et al., 1994). Documented in Fig. 10B is the homologous series (a series of compounds with both similar molecular formula and similar chemical properties) of normal n-alkenes and n-alkanes of n-C_9 to n-C_{16}, and up to C_{23} n-alkenes, with a ratio ~3 to 1 in favor of alkene (aliphatic unsaturated hydrocarbons). In contrast, Tegelaar et al. (1989) and McKinney et al. (1996) have shown an alkene-peak predominance. The alkaline solution of 8-ovule (Fig. 11A and B) shows very little pyrolytic information, where isoprene(5), 1-hexene(6), and heptene(9) are comparatively very small (compare with Figs. 11A or 10A).

5.2.2. Cupric V, and fossilized layer, 202-ovule

Fig. 12A to C, respectively. Cupric V shows quality low M.W. products (similar to 8-ovule in Fig. 10A), which are propene(1), 2-butene(2), toluene(10), and 2,4-octadiyne, noting that isoprene(5) and benzene (7) are not recorded, and that toluene(10) is present in comparatively

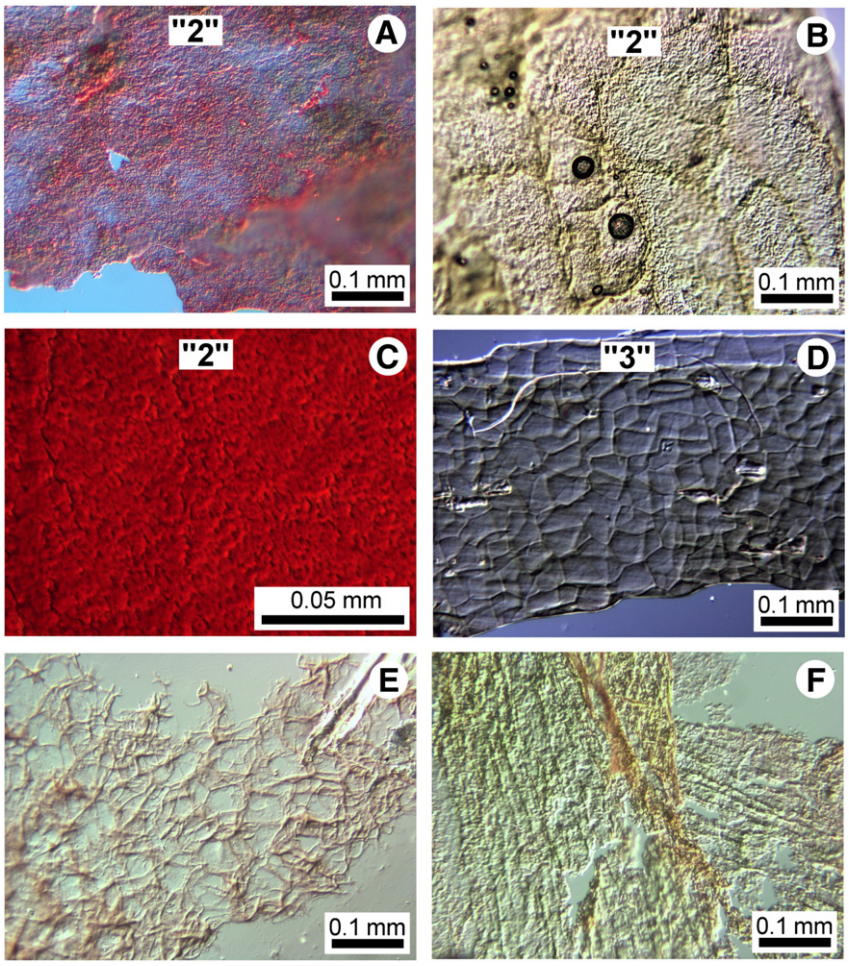

Fig. 7. *Trigonocarpus grandis*. 202-ovule. (A) to (C) "2" Granulose exine, noting that (C) is magnified x500. See text. Slides 85-202/20, 85-202/17, and 5-202/21, respectively. (D) "3" Cuticles of the outer integument. Slide 85-202/18. (E) Parenchymatuos cells. Slide 85-202/9. (F) Sclerenchymatous cells. Slide 85- 85- 202/10. See text for explanation of "2" and "3". Nomarski phase-contrast microscopy.

higher amounts. In the higher M.W. chromatograms (Fig. 12B and C) n-alkenes/n-alkanes are absent which confirms a non-cuticle state for the fossilized layer.

5.2.3. 3-258a ovule

The pyrolysates (Fig. 13A) from a chemically untreated coalified ovule with some preserved cuticle (cf. Fig. 9A) show an array of low M.W. products of which propene(1) and toluene(10) are the most prominent. The higher M.W. chromatogram (Fig. 13B) records branched C_{12} alkenes(17) and branched C_{14} alkenes(18), and the remaining pyrolysates—vinyl furan(12), m-cresol(13), o-cresol(l4), 3-Et phenol(15), and 2-Et phenol(16)—could be interpreted as pyrolytic markers of "fern" lignin.

5.3. ^{13}C CP/MAS NMR spectra

5.3.1. Coal

Coal-sample spectra are compared in Fig. 4, where each pair represents data from the Lloyd Cove and the Hub Seams, which document the well-separated aliphatic and aromatic carbon signals. Features in the aromatic range (between about 165 ppm to 100 ppm) are typical with their well-understood signatures of oxygen-substituted aromatic carbons around 154 ppm, the bridge aromatic carbons around 139 ppm, and protonated aromatic carbons around 127 ppm with shoulders around 120 ppm (Werner-Zwanziger et al., 2005 and references therein). The SSB intensities of these aromatic peaks around 3 ppm, mostly from the largest peak at 127 ppm, are indicated by a star *. Aliphatic signals resonate between 65 ppm to 3 ppm. The maxima at 20 ppm, and possibly a shoulder at 15 ppm, can be attributed to methyl-groups, whereas the other features resulted from linear chain and branching aliphatic carbons, and possibly from some methoxy carbons (lignin-related). The Lloyd Cove sample shows a small pronounced sharper peak with a maximum at 30 ppm attributed to linear chain-CH groups. This peak can be quite dominating in younger-aged coals (Werner-Zwanziger et al., 2005), but is quite weak and not visible at the longer contact times. In addition, the sample also shows a weak signal intensity at 74 ppm, stemming from alcohol-aliphatic carbons. The aromaticity ratios for a contact time of 0.5 ms $f = 0.55 \pm 0.03$ (Lloyd Cove coal), 0.56 ± 0.06 (Hub coal), and for contact time 1 ms, $f = 0.59 \pm 0.07$ (Lloyd Cove), 0.61 ± 0.04 (Hub coal).

5.3.2. T. grandis and A. pseudograndinioides ^{13}C CP/MAS NMR spectra

Fig. 14A and B shows the full spectra, and the two spectra that highlight the weaker signals, respectively of *A. pseudograndinioides*. The two spectra in Fig. 14B can be distinguished from one another based on their noise levels, where the signals from the cuticle of *A. pseudograndinioides* are more noisy (heavily zigzagging traces). Both spectra (Fig. 14A) are dominated by the strong aliphatic peak, with maxima around 30 ppm, i.e., aliphatic unsubstituted carbons

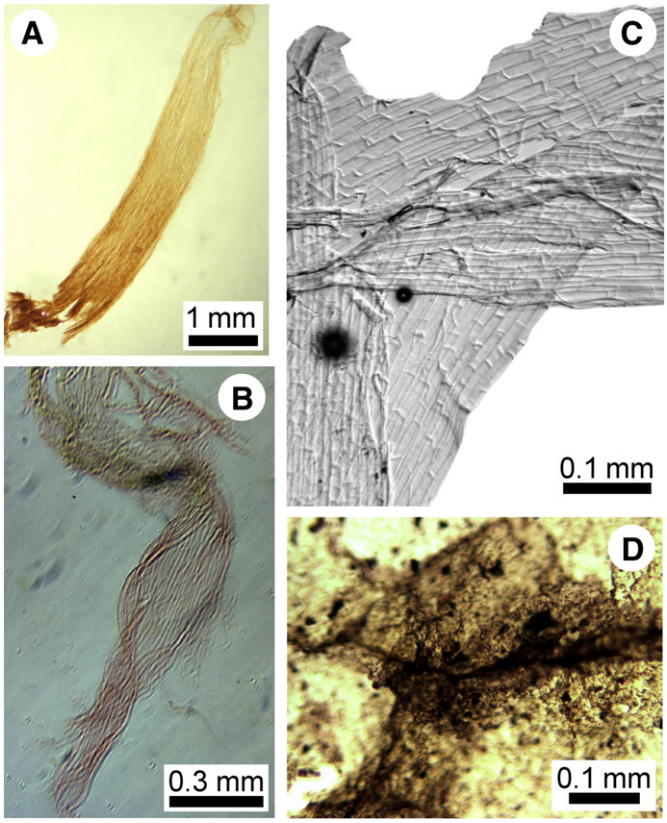

Fig. 8. *Trigonocarpus grandis*. 202-ovule, (A) to (C) Rib-related structures. (A) Isolated linear structure before maceration. Photographed immersed in water. (B) After macerating; *ca.* 1/3 of the structure is shown. Slide 85-202/1. Plane-polarized light. (C) Central part of (A) with elongate-cell structure. Slide 85-202/1. (D) Fossilized layer with cutinized, Y-shaped ridges. Slide 85-202/5. (B) to (D) Nomarski phase-contrast microscopy.

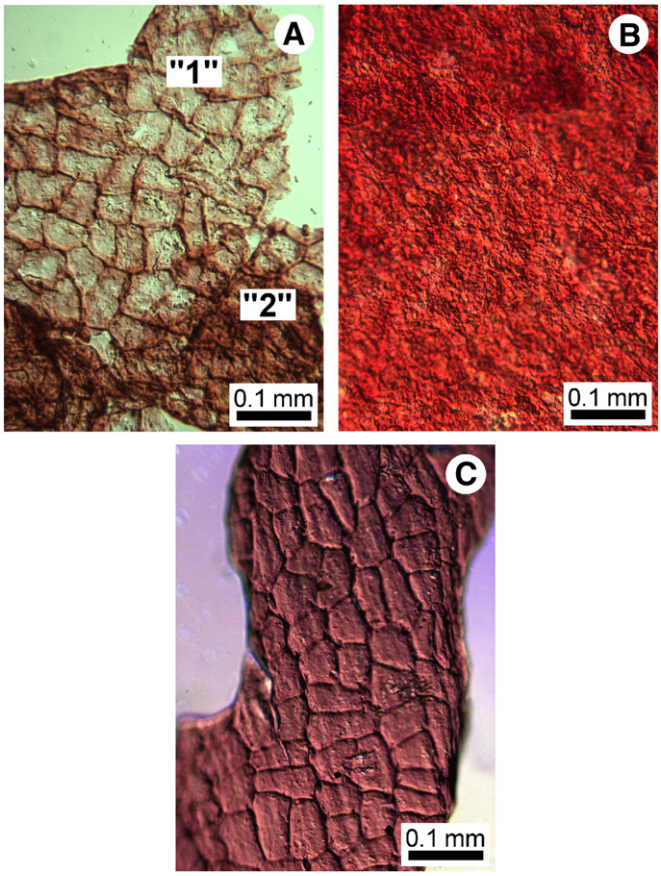

Fig. 9. *Trigonocarpus grandis*. (A) 3-258a: Cuticle with near-isodiametric cells. "1" single, "2" folded-over layer. Slide 03-258a/1. (B) 5-10/11-5: granulose megaspore membrane separated from (C). (C) Cuticle B. Inner? cuticle of the inner integument without diaphanous layer. Slides 5-10/11-5/1"1". Nomarski phase-contrast microscopy.

with the linear chain carbons resonating in the sharper peak. The latter is more pronounced in the cuticles of *A. pseudograndinioides*, which corroborates infrared results of cuticles (Zodrow and Mastalerz, 2007, Fig. 8).

Concerning the weaker signals, both organs show the full range of carbon-chemical shifts. In addition to the unsubstituted carbons assigned above, these groups are present:

(1) maxima near 62 ppm: CH_2-groups (methylene) from alcohols and ester
(2) maxima near 75 ppm: CH_2–O ether linkages CH
(3) near 85 ppm: C alcohol and ether linkages
(4) maxima near 104 ppm: acetal groups which are not present for *A. pseudograndinioides*
(5) near 171 ppm: aromatic resonances as described above, carboxyl groups, and
(6) near 200 ppm: aldehydes and ketones.

6. Discussion

6.1. Preservation comparison among the specimens, and what a coalified ovule is

Overall, the relative decreasing abundance of preserved structural components is as follows: cuticles, megaspore membranes, diaphanous layers, nucellar cuticle, followed by rare sclerenchymatous and parenchymatous tissues. Evidence for the integuments is possibly represented by the fossilized layer, and sclerotestal tissues (Figs. 5B, 7F, 8A to C). These could relate to the trigonous ribs (Taylor, 1965, p. 26), manifest as external-lithified impressions that are the basis for trigonocarpalean taxonomy (e.g., Brongniart, 1881, p. 39). Vasculature is apparently not preserved. However, taken as a whole, the microscopical data leave little doubt that not all specimens consistently preserved the same structures/tissues, nor to the same degree of quality. 3-258a ovule is an extreme as megaspore membranes and diaphanous layer are not preserved. The sum-total components from the variably preserved ovules present the nature of coalified ovules from Sydney, and by inference coalified ovules from other Carboniferous coalfields, if preserved under similar conditions.

6.1.1. Pyrolysates and original make-up of the T. grandis seed

These data offer a first attempt at deciphering aspects of original make-up of structural parts of Carboniferous ovules, highlighting at the same time limits of the Py-GC/MS methodology (Zodrow and Mastalerz, 2001, 2002 outlined advantages).

The homologous n-alkenes/n-alkanes series of cuticle A (8-ovule) suggests a cutin-based composition of hydrocarbon-chain structure. Analogous with "Most fossil cuticles [*sic* foliar] that reveal the presence of a macromolecule based on long-chain aliphatic moieties…." (van Bergen et al., 1994a, p. 144; Edwards et al., 1997, p. 348; Koch and Ensikat, 2008; Stoyko and Rudyk, 2013). The series is presumed to have arisen from the random pyrolysis of polyethylenic $(CH_2)_n$ chains that must be linked to the organic structures by bonds more stable than the ester linkages in extant cutin since such structures cleave preferentially to yield a carboxylic acid from the acyl moiety and an alkene from the alkyl moiety. Isoprene, probably in the 0.5 to 1.0% range (D'Angelo et al., 2010b), in agreement with van Bergen et al. (1994a), could have been derived from some tocopherol precursor as vitamin E-like compound. These results

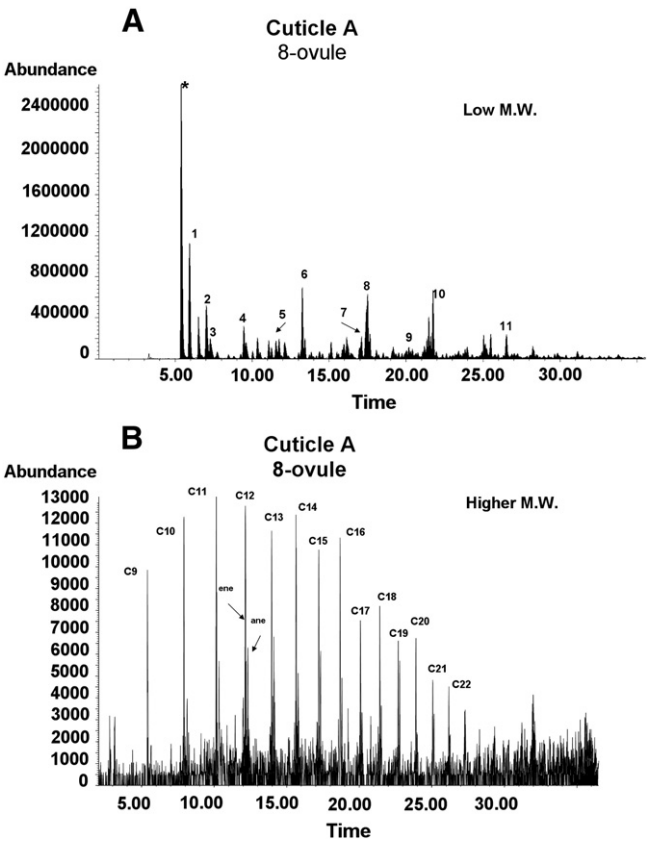

Fig. 10. Py-GC/MS. 8-ovule. Pyrolytic products. Cuticle of the inner integumentary surface. (A) Low M.W. (molecular weight), (B) Higher M.W. n-alkene/n-alkane products. Expansion of Y-axis for more accurate hydrocarbon observation. *CO_2 from air contamination, which also applies to Figs. 11 to 13. See Table 2 (supplementary data) for identification of products 1 to 19. ane = alkane, ene = alkene.

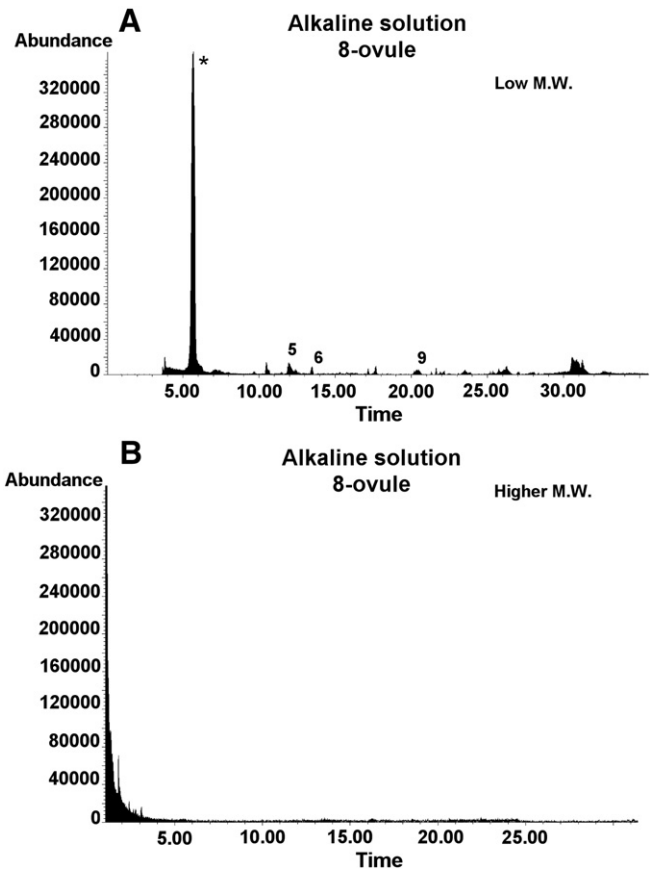

Fig. 11. Py-GC/MS. 8-ovule. Pyrolytic products. Alkaline solution. (A) Low M.W. (B) Higher M.W.

contrast with cupric V and the fossilized layer (202-ovule) that hardly yielded any pyrolytic information, though FTIR data indicate CH_2/CH_3 ratios (6–13) compatible with cutin (D'Angelo and Zodrow, 2011). This is likely due to interference caused by organic matter being macromolecular with small side-groups that are easily fragmented off to give products as in Fig. 12A. Alternatively, the macromolecules may be too cross-linked to give higher M.W. in Fig. 12B or C. Ovule 3-258a demonstrates that useful information relating to branched alkenes is possible from the vitrain of a compressed ovule.

In contrast with the informative IR data from alkaline solutions (Zodrow et al., 2009), the Py-GC/MS data show very little information which is likely the result of traces of the alkaline base that is known to severely influence the pyrolysis of any organic matter that is present. Alternatively, the results could just mean that the organic matter is a highly cross-linked, complex, macromolecule and that pyrolyzing it only produced char. These results emphasize the importance of using multiple analytical techniques when studying different sample forms (e.g., coalified ovule, alkaline solution, and cupric V) of fossil remains).

6.2. Comparison of the coalified with certain petrified ovules

6.2.1. Integumentary cuticles

Although we present detailed descriptions of cuticles, comparison with coal-ball cuticles is hindered as in the North American literature they are described but mostly inadequately figured (Arnold, 1948; Hoskins and Cross, 1946; Taylor, 1965; Zimmerman and Taylor, 1970). Darrah (1968), however, documented rectangular doublet (and quadruplet) cell topographies. We agree with the conveyance by these authors that integumentary cuticles have little or no taxonomic-systematic value. This, however, ignores the significance for the histochemical approach taken in this paper, which aids in elucidating molecular structure, and at the same time offering an explanation for the preservation.

6.2.2. Nucellus

Nucellar features are considered salient characteristics for comparing compressed (coalified) ovules with petrified seeds. Cleal et al. (2010, Pl. 3, Fig. 3) assigned large cells with granulose surfaces of 8-ovule to the nucellus. In this study, we refined the analysis and figured higher-resolution images for a more comprehensive comparison with the corresponding petrified materials. This includes first of all the similarity of the topical features between the coalified "type" specimen in Fig. 5H and the petrified seed in Fig. 5I, i.e., clear outlines of nucellar cells and cuticles by prominent ridges, and granulose exine surfaces (Zimmerman and Taylor, 1970, pl. 2, Fig. 4 ×178). The similarity of granulose megaspore membrane is highlighted for our specimens (×125 and ×500 magnifications) on comparison with Darrah's exine image of *P. gigantea* (1968, pl. 2, Fig. 8: transmitted light, ×225). The comparison indicates minimal differences.

Darrah (1968) emphasized that in petrified *P. gigantea*, *P. vera*, *P. composita*, *P. stewartii*, and *P. saharaspermum* only two-layered megaspore membranes occur (demonstrably established via coal-ball sectioning), the same as was observed in older coalified *Trigonocarpus* (Pettitt, 1966, pl. 18, Fig. 3; p. 251). Our data conform with these observations. We infer from the one or three megaspore membranes that we reported remnants of a two-layered megaspore membrane for *T. grandis*. We add that work on the two-layered megaspore membrane is still in progress, confirming a two-layered membrane.

In addition, nucellus-cell sizes are also considered comparable parameters, though not of crucial importance. The nucellar cuticle must be distinguished from the inner nucellar layer, where the former has

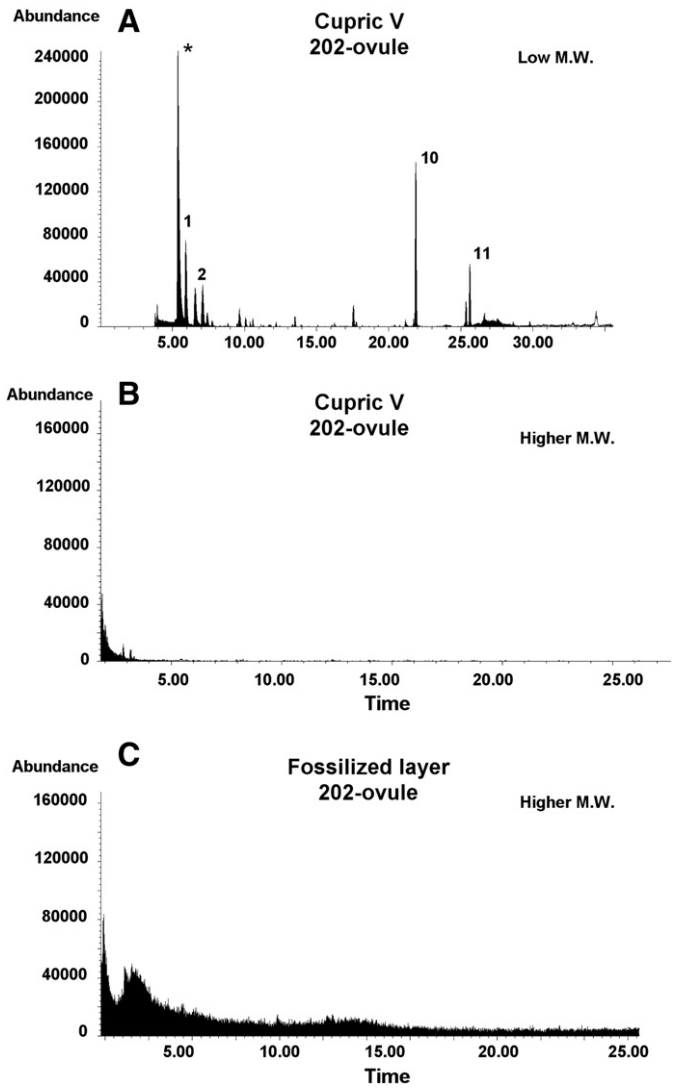

Fig. 12. Py-GC/MS. 202-ovule. Pyrolytic products. Cupric V and fossilized layer. (A) Low M.W. of cupric V (see Fig. 3C). (B) Higher M.W. of cupric V. (C) Higher M.W. of fossilized layer (see Fig. 8D), noting that the low M.W. pyrolytic products are similar to those of (A).

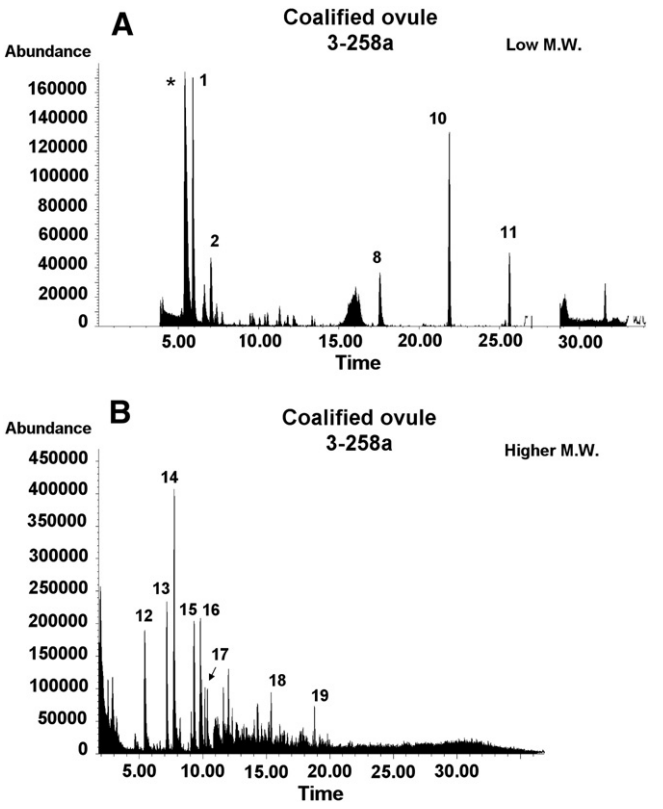

Fig. 13. PY-GC/MS. 3-258a. Pyrolytic products. Coalified ovule. (A) Low M.W. (B) Higher M.W.

thick cutinized anticlinal walls, diaphanous luminae, and larger cell sizes that range between 200 and 230 μm in length and 150 and 230 μm in width. What we think represent measurements of the inner nucellar layer range between 53 and 240 μm in length and 40 and 230 μm width, which broadly compare with 115 μm to 175 μm reported by Hoskins and Cross (1946, Fig. 17B, p. 223)"… giving us another character by which to identify it [*sic* nucellus]". Taylor (1965, p. 25–26) reported a nucellar thickness of up to 1.7 mm for *P. gigantea*, isodiametric cells 70 μm to 13 μm (compare Darrah, 1968, Table 2: 177 μm by 104 μm), and referenced even larger cells (110 μm to 400 μm) as being nucellar tissue in the pollen-chamber region. The point is made that nucellar cells are considerably larger and of different configuration than those of the cuticles, and measurements on our specimens conform with the observations from the petrified specimens.

6.3. T. grandis–A. pseudograndinioides "linkage"

Given the widely different maceration times for 8-ovule (20 d), and only up to 168 h for *A. pseudograndinioides*, the similarity of their spectra is quite remarkable. Schulze's process has probably oxidized all available chemical species and the final products are presumably determined by the original chemical structure of the fossil plant. The inference is based on controlled time-maceration experiments with foliage of *A. pseudograndinioides*, where increased maceration time to 168 h did not substantially affect oxygenated groups, as determined by FTIR experiments (Zodrow and Mastalerz, 2007). Despite ^{13}C CP/MAS NMR spectral similarities, indicative of the differences of the original plant materials is the intensity

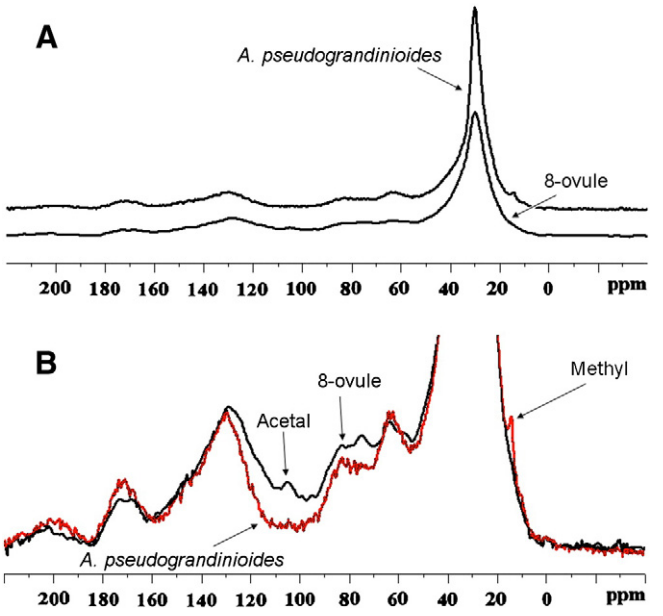

Fig. 14. ^{13}C CP/MAS NMR spectra: cuticle of *Alethopteris pseudograndinioides* and cuticle of the inner surface of the integument of 8-ovule. (A) Full traces of high aliphatics. (B) Highlights of weaker signals.

difference in the unbranched CH_2 groups, and the small, but very sharp methyl-group peak at 13.8 ppm in the cuticles of *A. pseudograndinioides* (Fig. 14). Methyl groups in this chemical-shift range are the terminating groups of unbranched chains. Missing the sharper component, 8-ovule has a broader resonance in this spectral region which is caused by less mobile or higher branched, unstructured aliphatic groups, showing higher networks. Also remarkable, and not observed in other cuticles of Carboniferous seed-fern species we have studied so far, is the peak at 10 ppm (U. Werner-Zwanziger, Banghao Chen and E. Zodrow 2008–2009. Unpublished ^{13}C CP/MS NMR research notes). Carbon signals at these shifts result from acetal groups, for example from polysaccharides that are the chemical building blocks of cellulose and starch, i.e., the structural components or energy-storage materials of plants (Nip et al., 1989). These signals from 8-ovule indicate that its tissues were part of the stronger, structurally relevant ovular tissue rather than the protective surface layer (cuticle) of the leaves of *A. pseudograndinioides*. The sharp methyl-group signal of *A. pseudograndinioides* and the stronger unbranched CH_2 groups, on the other hand, indicate longer, linear chains and thereby a hydrophobic, oily or waxy cuticular structure (van Bergen et al., 2004; Zodrow et al., 2009, Fig. 3, for a molecular presentation of the cutan biopolymer).

In summary, we caution that especially the ketones, acids, oxygenated and hydroxygenated carbons may have been introduced during Schulze's maceration process (U. Werner-Zwanziger, Banghao Chen and E. Zodrow 2008–2009. Unpublished ^{13}C CP/MS NMR research notes). Differences between the spectra of the 8-ovule and the associate pinnule cuticle of *A. pseudograndinioides* are seen in the higher intensity of the sharper linear-chain signals in the pinnule spectrum (around 30 ppm), the methyl peak (around 13.8 ppm) which is absent in the 8-ovule spectrum, and the acetal peak (104 ppm) in the 8-ovule spectrum which is missing in the pinnule data set.

The assumption that cuticle A represents part of the outer integument (cupule), thought to be homologous with laminate foliage, requires further study as the morphological interpretation by Cleal et al. (2010) is "inner cuticle of the inner integument". However, the approach for "connecting" isolated ovules with physically associated foliage by chemical similarity is a testable hypothesis for which pitfalls that concern circumscribing "chemical similarity" have to be ironed-out. The alternative to this modus operandi is relying on serendipitous finds of organically connected ovules that, however, after more than 100 years of collecting world-wide (Wagner, 1968) yielded only three or so ovules of the smaller types that are indisputably attached to foliage (cf. Retallack and Dilcher, 1988; Zodrow and McCandlish, 1980).

7. Concluding remarks

Seldom can it be said for a group of Carboniferous plant organs, preserved as compressions, coal balls, and fossilized-cuticles, that morphology, histology and chemical aspects have been so thoroughly studied as for these larger medullosalean ovules. Preservation in coalified ovules is likely favored by original seed chemistry which is inferred from cuticle A (normal or linear alkene/alkane series), and can probably be said to apply to integumentary cuticle (epidermises), megaspore membranes, diaphanous layers, and nucellar cuticle as well. Supportive in this respect are ^{13}C CP/MAS NMR data. By the same token, namely vasculature, fleshy seed coats, and sclerotestal material are not, or poorly preserved. Preservation variability among the specimens, despite near-identical maturity levels in the sample section, is ascribed to factors that override aliphatic chemistry, possibly clay-diagenesis effects combined with variable Eh–pH conditions (cf. Krumbein and Garrels, 1952; van Bergen et al., 1994b).

A practical implication is the chemotaxonomic potential based on aliphatic chemistry, as indeed has been concluded previously by Osborne et al. (1993) for some extant gymnospermous cycadean foliage. Koch and Ensikat (2008) experimentally underpin the implication. Initial evidence suggests that cuticular topography and diaphanous layers have the potential for differentiating integuments, i.e., decide when inner/outer integuments are at issue. Not overlooked either can be ovules as a potential kerogen source, given the vast extent of Carboniferous medullosalean forests and prodigious productions as attested to by the fossil record (e.g. Arnold, 1938).

Unlike coal-ball formation by carbonate-replacement chemistry (summary Zodrow et al., 2002; Raymond et al., 2012) for preserving seed structures in the finest detail, formation of coalified ovules is different, and its complexity is probably far from being understood. The decidedly variable maceration times to produce workable surfaces likely reflect the complex history of formation. The compression process ostensibly preserved sufficient seed structure/tissue components for comparison with the larger *Pachytesta* species. And the two-layered granulose exine megaspore membrane is cited evidence for a generic union. We note that what we illustrate as diaphanous layer bears topographical resemblance with a tectum as illustrated by Zimmerman and Taylor (1970, Pl. 6, Figs. 1 and 5), but the fossilized layer is difficult to correlate with coal-ball seeds. The challenge that remains is how does the chemical make-up of pachytestal tissues compare for a detailed description of the pathways of organic matter transformations with coalified ovules?

Test results of the novel modus operandi, re. organ–organ linkage, are encouraging for a budding scientific branch whose overall aim is intended to promote whole plant-fossil reconstruction of which connective anatomy is an important component (Dilcher, 1991). But more data for organ–organ testing of homologous structures by various spectrometric methods are necessary for a sound scientific theory.

In summary, *T. grandis* is considered the seed of *A. pseudograndinioides*, although where attachment occurred to the mother tree remains unknown. Anatomically it is described as a seed having inner and outer integuments and a two-layered nucellus with granulose exine, covered by nucellar cuticles and diaphanous layers.

Acknowledgements

Drs. M. Katherine Jones (Biology), D. Keefe (Molecular Spectroscopy Laboratory), and M. Bierenstiel (Chemistry Department) of the Cape Breton University provided invaluable assistance by making available microscopes, FTIR instruments, and research literature; J. Pšenička (West Bohemian Museum, Czech Republic), found and donated ovule 3-258a to the Palaeobotanical Collection, Cape Breton University; M. Mastalerz (Indiana Geological Survey/Indiana University) provided the vitrinite reflectance data; more importantly she suggested restructuring the MS as we did, and C.J. Cleal, National Museum Wales, located research literature. The journal reviewers, Drs. I. Sýkorová (Academy of Sciences of the Czech Republic), W. A. DiMichele (Smithsonian Institution), and an anonymous reviewer proposed significant changes which improved the quality of presentation of the MS. We are grateful for their efforts and thank them all cordially and collegially. Some financial support for this ongoing research program from the Universidad Nacional de Cuyo (SeCTyP, Project 06/M038) is acknowledged.

Supplementary data

Supplementary data to this article can be found online at http://dx.doi.org/10.1016/j.coal.2013.01.013.

References

Arnold, C.A., 1938. Paleozoic seeds. The Botanical Review 5, 205–234.
Arnold, C.A., 1948. Some cutinized seed membranes from the coal-bearing rocks of Michigan. Bulletin of the Torrey Botanical Club 75, 131–146.

Berns, A.E., Conte, P., Pohlmeier, A., Alonzo, G., 2011. Preface to the Special Issue on "Applications and development of magnetic resonance techniques in geosciences". Organic Geochemistry 42, 865–866.
Birk, D., 1990. Quantitative coal mineralogy of the Sydney Coalfield, Nova Scotia, Canada, by scanning electron microscopy, computerized image analysis, and energy-dispersive X-ray spectrometry. Canadian Journal of Earth Sciences 27, 163–179.
Brongniart, A., 1881. Recherches sur les grains fossils silicifiées. Masson, Paris, p. 93.
Cleal, C.J., Zodrow, E.L., Mastalerz, M., 2010. An association of *Alethopteris* foliage, *Trigonocarpus* ovules and *Bernaultia*-like pollen organs from the Middle Pennsylvanian of Nova Scotia Canada. Palaeontographica Abteilung B 283, 73–97.
D'Angelo, J.A., Zodrow, E.L., 2011. Sample forms of ovular preservation: Chemometric study of functional groups in *Trigonocarpus grandis* (Pennsylvanian seed fern, Canada). Organic Geochemistry 42, 1039–1054.
D'Angelo, J.A., Zodrow, E.L., Camargo, A., 2010a. Chemometric study of functional groups in Pennsylvanian gymnosperm plant organs (Sydney Coalfield, Canada): Implications for chemotaxonomy and assessment of kerogen formation. Organic Geochemistry 41, 1312–1325.
D'Angelo, J.A., Werner-Zwanziger, U., Helleur, R., Zodrow, E.L., 2010b. Molecular characterization of a seed-fern ovule (Pennsylvanian, Sydney Coalfield, Canada). X Congreso Argentino de Paleontología y Bioestratigrafía, VII Congreso Latinoamericano de Paleontología, La Plata, Argentina- Septiembre de 2010. Sesiones Libres, p. 155.
Darrah, E.L., 1968. The microstructure of some Pennsylvanian seeds and megaspores studied by maceration. Micropaleontology 14, 87–104.
De Sloover, J.L., 1964. Études sur les Cycadales. III. Nucelle, gaméophyte femelle et embryon chez Encephalartos poggei Asch. Cellule 64, 149–200.
Dilcher, D.L., 1991. The importance of anatomy and whole plant reconstructions in palaeobotany. Current Science 61, 627–629.
Edwards, D., Ewbank, G., Abbott, G.D., 1997. Flash pyrolysis of the outer cortical tissues in Lower Devonian *Psilophyton dawsonii*. Botanical Journal of the Linnean Society 124, 345–360.
Favre-Duchartre, M., 1956. Contribution à l'étude de la reproduction chez le *Ginkgo bilboa*. Revue Cytologie Biologique vegetales 17, 1–218.
Gastaldo, R.A., Matten, L.C., 1978. *Trigonocarpus leeanus*. A new species from the Middle Pennsylvanian of southern Illinois. American Journal of Botany 65, 882–890.
Gibling, M.R., Bird, D.J., 1994. Late Carboniferous cyclothems and alluvial paleovalleys in the Sydney Basin, Nova Scotia. Bulletin of the Geological Society of America 106, 105–117.
Hacquebard, P.A., 1993. The Sydney Coalfield of Nova Scotia. International Journal of Coal Geology 23, 29–42.
Hacquebard, P.A., 1998. Petrographic, physico-chemical, and coal facies studies of ten major seams of the Sydney Coalfield of Nova Scotia. Bulletin Geological Survey of Canada, Ottawa 520.
Hacquebard, P.A., Donaldson, J.R., 1970. Coal metamorphism and hydrocarbon potential in the Upper Paleozoic of the Atlantic Provinces. Canadian Journal of Earth Sciences 7, 1139–1163.
Hartgens, W.A., Sinninghe Damsté, J.S., De Leeuw, J.W., 1994. Geochemical significance of alkylbenzene distribution in ash pyrolysates of kerogen, coals, and asphalts. Geochimica et Cosmochimica Acta 58, 1759–1775.
Hatcher, P., Lerch III, H.E., Verheyen, T.V., 1989. Organic geochemical studies of the transformations of gymnospermous xylem during peatification and coalification to subbituminous coal. International Journal of Coal Geology 13, 65–97.
Hoskins, J.H., Cross, A.T., 1946. Studies in the Trigonocarpales. Pt I. *Pachytesta vera*, a new species from the Des Moines Series of Iowa. American Midland Naturalist 36, 207–250.
Knicker, H., 2011. Solid state CPMAS ^{13}C and ^{15}N NMR spectroscopy in organic geochemistry and how spin dynamics can either aggravate or improve spectra interpretation. Organic Geochemistry 42, 867–890.
Koch, K., Ensikat, H.J., 2008. The hydrophobic coatings of plant surfaces: Epicuticular wax crystals and their morphologies, crystallinity and molecular self-assembly. Micron 39, 759–772.
Krumbein, W.C., Garrels, R.M., 1952. Origin and classification of chemical sediments in terms of pH and oxidation-reduction potentials. Journal of Geology 52, 1–33.
Lesquereux, L., 1884. Description of the Coal Flora of the Carboniferous Formation in Pennsylvanian and Throughout the United States. Board of Commissioneres, Second Geological Survey, Harrisburg: Second Geological Survey of Pennsylvania, Report of Progress, p. 695-977 (pls. 88-111).
Lyons, P.C., Orem, W.H., Mastalerz, M., Zodrow, E.L., Vieth-Redemann, A., Bustin, R.M., 1995. ^{13}C NMR, micro-FTIR and fluorescence spectra, and pyrolysis-gas chromatograms of coalified foliage of late Carboniferous medullosan seed ferns, Nova Scotia, Canada: Implications for coalification and chemotaxonomy. International Journal of Coal Geology 27, 227–248.
McKinney, D.E., Bortiatynski, J.M., Carson, D.M., Clifford, D.J., de Leeuw, J.W., Hatcher, P.G., 1996. Tetramethylammonium hydroxide (TMAH) thermochemolysis of the aliphatic biopolymer cutan: insights into the chemical structure. Organic Geochemistry 24, 641–650.
Meyen, S.V., 1984. Basic features of gymnosperm systematics and phylogeny as evidenced by the fossil record. The Botanical Review 50, 1–111.
Nip, M., De Leeuw, J.W., Schenk, P.A., 1989. Flash pyrolysis and petrographic study cutinite from the Indiana paper coal. Geochimica et Cosmochimica Acta 53, 671–683.
Oliver, F.W., 1903. The ovules of the older Gymnosperms. Annals of Botany XVII, 451–578.
Osborne, R., Salatino, A., Salatino, M.L.F., Sekiya, S.M., Vazquez-Torres, M., 1993. Alkanes of foliar epicuticular waxes from five cycad genera in the Zemiaceae. Phytochemistry 33, 607–609.
Pettitt, J.M., 1966. Exine structure in some fossil and recent spores and pollen as revealed by light and electron microscopy. Bulletin of the British Museum (Natural History) Geology 13 (4), 221–257 (plus 21 pls).
Raymond, A., Guillemette, R., Jones, C.P., Ahr, W.M., 2012. Carbonate petrology and geochemistry of Pennsylvanian coal balls from the Kalo Formation of Iowa. International Journal of Coal Geology 94, 137–149.
Retallack, G.J., Dilcher, D.L., 1988. Reconstructions of selected seed ferns. Missouri Botanical Garden 75, 1010–1057.
Rothwell, G.W., 1985. The role of comparative morphology and anatomy in interpreting the systematics of fossil gymnosperms. The Botanical Review 51, 319–327.
Schulze, F., 1855. Bemerkungen über das Vorkommen wohlerhaltener Cellulose in Braunkohle and Steinkohle. Berliner Königlicher Akademie der Wissenschaften Sitzungsbericht 20, 676–678.
Sporne, K.R., 1974. The morphology of gymnosperms, 2nd ed. Hutchison University Library, London (216 pp.).
Stoyko, S.S., Rudyk, B.W., Mar, A., Zodrow, E.L., D'Angelo, J.D., 2013. Powder X-ray diffraction and X-ray photoelectron spectroscopy of cutin from a 300 Ma tree fern (Alethopteris pseudograndinioides, Canada). International Journal of Coal Geology 106, 35–38.
Taylor, T.N., 1965. Paleozoic seed studies: A monograph of the American species of *Pachytesta*. Palaeontographica Abteilung B 117, 1–46.
Tegelaar, E.W., de Leeuw, J.W., Derenne, S., Largeau, C., 1989. A reappraisal of kerogen formation. Geochimica et Cosmochimica Acta 53, 3103–3106.
Thomas, B.A., Spicer, R.A., 1987. The Evolution and Palaeobiology of Land Plants. Croom Helm, London (309 pp.).
van Bergen, P.F., Collinson, M.E., Simninghe Damsté, J.S., de Leeuw, J.W., 1994a. Chemical and microscopical characterization of inner seed coals in fossil water plants. Geochimica et Cosmochimica Acta 58, 231–239.
van Bergen, P.F., Collison, M.E., Hatcher, P.G., de Leeuw, J.W., 1994b. Lithological control on the state of preservation of fossil seed coats of water plants. Organic Geochemistry 22, 683–702.
van Bergen, P.F., Blokker, P., Collinson, M.E., Sinninghe Damsté, J.S., de Leeuw, J.W., 2004. Structural biomocromolecules in plants: what can be learnt from the fossil record. In: Hemsley, A.R., I Poole, I. (Eds.), The Evolution of Plant Physiology. Elsevier Academic Press, Oxford, pp. 133–154.
Wagner, R.H., 1968. Upper Westphalian and Stephanian species of *Alethopteris* from Asia Minor and North America. Uitgevers-Maatschappij. Ernest Van Aelst, Maastricht (318 pp.).
Werner-Zwanziger, U., Lis, G., Mastalerz, M., Schimmelmann, A., 2005. Thermal maturity of type II kerogen from the New Albany Shale assessed by ^{13}C CP/MAS NMR. Solid State NMR 27, 140–148.
Werner-Zwanziger, U., Banghao Chen, Zodrow, E.L., 2008–2009. ^{13}C NMR experiments with seed-fern cuticles. Sydney Coalfield, Cape Breton University. Unpublished spectra.
Zodrow, E.L., 1977. Carboniferous Fossil Flora of Sydney Coalfield, Nova Scotia. Accession v. II. p. 151. Cape Breton University. Unpublished report.
Zimmerman, R.P., Taylor, T.N., 1970. The ultrastructure of Paleozoic megaspores membranes. Pollen et Spores 12 (3), 451–468.
Zodrow, E.L., 1987. Geochemical trends in whole-seam coal channel samples from the Sydney Coalfield (Upper Carboniferous), Nova Scotia, Canada. Maritime Sediments and Atlantic Geology 23, 141–150.
Zodrow, E.L., 2002. The "medullosalean forest" at the Lloyd Cove Seam (Pennsylvanian, Sydney Coalfield, Nova Scotia). Atlantic Geology 38, 177–195.
Zodrow, E.L., 2004. Note on different kinds of attachments in trigonocarpalean (Medullosales) ovules from the Pennsylvanian Sydney Coalfield, Canada. Atlantic Geology 40, 197–206.
Zodrow, E.L., 2007. Reconstructed tree fern *Alethopteris zeilleri* (Carboniferous, Medullosales). International Journal of Coal Geology 69, 68–89.
Zodrow, E.L., Cleal, C.J., 1985. Phyto- and chronostratigraphical correlations between the late Pennsylvanian Morien Group (Sydney, Nova Scotia) and the Silesian Pennant Measures (south Wales). Canadian Journal of Earth Sciences 22, 1465–1473.
Zodrow, E.L., Cleal, C.J., 1998. Revision of the pteridosperm foliage *Alethopteris* and *Lonchopteris* (Upper Caboniferous), Sydney Coalfield, Nova Scotia. Canada. Palaeontographica Abteilung B 267, 65–122.
Zodrow, E.L., Mastalerz, M., 2001. Chemotaxonomy for naturally macerated tree-fern cuticles (Medullosales and Marattiales), Carboniferous Sydney and Mabou Sub-Basis, Nova Scotia, Canada. International Journal of Coal Geology 47, 255–275.
Zodrow, E.L., Mastalerz, M., 2002. FTIR and Py-GC-MS spectra of true-fern and seed-fern sphenopterids (Sydney Coalfield, Nova Scotia, Canada, Pennsylvanian). International Journal of Coal Geology 51, 111–127.
Zodrow, E.L., Mastalerz, M., 2007. Functional groups in a single pteridosperm species: Variability and circumscription (Pennsylvanian, Nova Scotia, Canada). International Journal of Coal Geology 70, 313–324.
Zodrow, E.L., McCandlish, K., 1980. On a *Trigonocarpus* species attached to *Neuropteris* (*Mixoneura*) *flexuosa* from Sydney Coalfield, Cape Breton Island, Nova Scotia, Canada. Review of Palaeonbotany and Palynology 30, 57–66.
Zodrow, E.L., Snigirevskaya, N.S., Palmer, C.A., 2002. Palaeoenvironments, carbonate processes in plant-tissue preservations of calcite coal balls: Donets Basin Russia and the Ukraine (Middle Carboniferous). Internatational Congress Carboniferous and Permian XIV, Calgary Aug. 17-21: Canadian Society of Petroleum Geologists, Memoir, 19, pp. 393–411.
Zodrow, E.L., Tenchov, Y.K., Cleal, C.J., 2007. The arborescent *Linopteris obliqua* plant (Medullosales, Pennsylvanian). Bulletin of Geosciences 82, 51–84.
Zodrow, E.L., D'Angelo, J.A., Mastalerz, M., Keefe, D., 2009. Compression-cuticle relationship of seed ferns: Insights from liquid-solid FTIR (Late Palaeozoic- Early Palaezoic, Canada-Spain-Argentina). International Journal of Coal Geology 79, 61–73.
Zodrow, E.L., D'Angelo, J.A., Mastalerz, M., MS, 2012. Histochemical synthesis: coalified *Trigonocarpus grandis* (Late Pennsylvanian seed-fern ovule, Canada).